Steroids 115 (2016) 160–168

Contents lists available at ScienceDirect

Steroids

journal homepage: www.elsevier.com/locate/steroids

Synthetic stigmasterol derivatives inhibit capillary tube formation, herpetic corneal neovascularization and tumor induced angiogenesis Antiangiogenic stigmasterol derivatives

Flavia M. Michelini [a,1], María Gabriela Lombardi [b,1], Carlos A. Bueno [a,1], Alejandro Berra [c,1], María Elena Sales [b,1], Laura E. Alché [a,*,1]

[a] Universidad de Buenos Aires, Facultad de Ciencias Exactas y Naturales, Departamento de Química Biológica, Laboratorio de Virología, Consejo Nacional de Investigaciones Científicas y Técnicas, Instituto de Química Biológica de la Facultad de Ciencias Exactas y Naturales (IQUIBICEN), Pabellón 2, 4to. piso, Ciudad Universitaria, C1428EGA Buenos Aires, Argentina

[b] Universidad de Buenos Aires, Facultad de Medicina, Segunda Cátedra de Farmacología, Consejo Nacional de Investigaciones Científicas y Técnicas, Centro de Estudios Farmacológicos y Botánicos (CEFYBO), Paraguay 2155 Piso 16°, C1121ABG Buenos Aires, Argentina

[c] Universidad de Buenos Aires, Facultad de Medicina, Departamento de Patología, Laboratorio de Investigaciones Oculares, J. E. Uriburu 950, EP, C1114AAD Buenos Aires, Argentina

ARTICLE INFO

Article history:
Received 5 April 2016
Received in revised form 21 July 2016
Accepted 2 September 2016
Available online 10 September 2016

Keywords:
Stigmasterol derivative
Neovascularization
HUVEC
Antiangiogenic activity
VEGF
Tumor
Herpetic keratitis

ABSTRACT

Angiogenesis plays a critical role in initiating and promoting several diseases, such as cancer and herpetic stromal keratitis (HSK). Herein, we studied the inhibitory effect of two synthetic stigmasterol derivatives on capillary tube-like structures and on cell migration in human umbilical vein endothelial cells (HUVEC): (22*S*,23*S*)-22,23-dihydroxystigmast-4-en-3-one (compound **1**) and (22*S*,23*S*)-3β-bromo-5α,22,23-trihydroxystigmastan-6-one (compound **2**). We also studied their effect on VEGF expression in IL-6 stimulated macrophages and in LMM3 breast cancer cells. Furthermore, we investigated the antiangiogenic activity of the compounds on corneal neovascularization in the murine model of HSK and in an experimental model of tumor-induced angiogenesis in mice.

Both compounds inhibited capillary tube-like formation, but only compound **1** restrained cell migration. Compound **1**, unlike compound **2**, was able to reduce VEGF expression. Only compound **1** not only reduced the incidence and severity of corneal neovascularization, when administered at the onset of HSK, but it also restrained the development of neovascular response induced by tumor cells in mice skin.

Our results show that compound **1** inhibits angiogenesis *in vitro* and *in vivo*. Therefore, compound **1** would be a promising drug in the treatment of those diseases where angiogenesis represents one of the main pathogenic events.

1. Introduction

Angiogenesis is an essential process in both embryonic development and adulthood that if not tightly regulated, it frequently becomes imbalanced and it is then associated with several pathological situations [1,2]. In this sense, angiogenesis leads to tumor neovascularization by promoting tumor growth and metastatic spread [3]. Particularly, vascular endothelial growth factor-A (VEGF-A) is primarily responsible for the "angiogenic switch" that allows tumor to grow and invade surrounding tissue [4–6]. Interleukin-6 (IL-6) is another mediator of angiogenesis in inflammatory and malignant conditions that stimulates the production of VEGF-A [7].

Another example of pathological angiogenesis can be found in Herpetic stromal keratitis (HSK), the first cause of infectious blindness in developed countries, which is caused by the infection of Herpes simplex virus type 1 (HSV-1) in the cornea [8]. The emergence of this HSV-1-induced ocular disease correlates with the development of corneal vascularization, normally avascular [9]. Polymorphonuclear cells (PMN) invade the cornea through new vessels and clear the virus but, at the same time, they enable the entry to various inflammatory cells and factors that provoke corneal scarring [8].

* Corresponding author at: Laboratorio de Virología, Departamento de Química Biológica, Facultad de Ciencias Exactas y Naturales, Universidad de Buenos Aires, Pabellón 2, 4to. piso, Intendente Güiraldes 2160, Ciudad Universitaria, C1428EGA Buenos Aires, Argentina.

E-mail address: lalche@qb.fcen.uba.ar (L.E. Alché).

[1] All authors are research members of the Consejo Nacional de Investigaciones Científicas y Técnicas (CONICET).

http://dx.doi.org/10.1016/j.steroids.2016.09.001
0039-128X/

We have reported that some 28-homobrassinosteroid analogues have *in vitro* antiviral activity against several viruses [10–15]. Two of them, (22*S*,23*S*)-22,23-dihydroxystigmast-4-en-3-one (compound **1**) and (22*S*,23*S*)-3β-bromo-5α,22,23-trihydroxystigmastan-6-one (compound **2**) (Fig. 1) prevent HSV-1 multiplication and reduce TNF-α and IL-6 secretion [16–20]. Both compounds strongly decrease the incidence and severity of HSK in the murine model of HSV-1 corneal infection [16,19,20]. Many natural brassinosteroids (BRs), such as brassinolide and *S,S*-homobrassinolide, that significantly inhibit the formation of capillary tubes in endothelial cells have been reported [21].

Since IL-6 is involved in neovascularization, which is crucial for the development of HSK and, besides, compounds **1** and **2** restrain IL-6 secretion *in vitro* and also reduce the signs of HSK, we decided to investigate their potential antiangiogenic activity on capillary tube-like structure formation in HUVEC and on VEGF expression [16–20]. Likewise, we also studied their antiangiogenic effect on tumor-induced angiogenesis and neovascularization in HSK.

2. Materials and methods

2.1. Cells, viruses, compounds and animals

Murine macrophage cell line J774A.1 (ATCC® Number TIB-67TM) was kindly provided by Dr. Osvaldo Zabal, from Instituto Nacional de Tecnología Agropecuaria (I.N.T.A.), Buenos Aires, Argentina, and it was grown in RPMI 1640 medium supplemented with 10% inactivated fetal bovine serum (FBS) (RPMI 10%) and maintained in RPMI supplemented with 2% inactivated FBS (RPMI 2%).

Human Umbilical Vein Endothelial Cells (HUVECs) were obtained from InVitrogen Argentina S.A. (catalog number C-003-5C), Buenos Aires, Argentina, and they were propagated and maintained in Medium 200 supplemented with Low Serum Growth Supplement (LSGS).

The LMM3 cell line was derived from the parental metastatic MM3 murine adenocarcinoma aroused in BALB/c mice in the Instituto de Oncología Angel H. Roffo, (Universidad de Buenos Aires, Argentina), and it was cultured in DMEM/F12 medium with 2 mM L-glutamine, 80 μg/ml gentamycin, supplemented with 10% FBS (Internegocios S.A., Buenos Aires, Argentina).

Five to seven-week-old male BALB/c mice purchased from I.N.T.A. (Buenos Aires, Argentina) were used in the HSK model. For the tumor-induced angiogenesis assay, we worked with three-month-old female BALB/c mice, obtained from the Facultad de Veterinaria, Universidad de Buenos Aires (CABA, Argentina). All mice were handled according to the Animal Care Guidelines from the National Institute of Health (USA) and the Association for Research in Vision and Ophthalmology (ARVO, USA). The protocol was approved by the Comisión Institucional para el Cuidado y Uso de Animales de Laboratorio (CICUAL), Facultad de Ciencias Exactas y Naturales (FCEyN), Universidad de Buenos Aires, that follows EU Directive 2010/63/EU for animal experiments.

Compounds **1** and **2** were dissolved in dimethylsulfoxide (DMSO) and diluted with culture medium. The maximum concentration of DMSO tested was 1% and exhibited no cytotoxicity under experimental conditions.

Anti-VEGF antibody bevacizumab (Avastin) was obtained from Roche Laboratories, San Francisco, USA.

2.2. Cytotoxicity assay

Cell viability was determined using the cleavage of the tetrazolium salt MTT (3-(4,5-dimethylthiazol-2-yl)-2,5-diphenyltetrazolium bromide) (Sigma, St. Louis, USA) by the mitochondrial enzyme succinate dehydrogenase to give a blue product (formazan), according to the manufacturer's instructions.

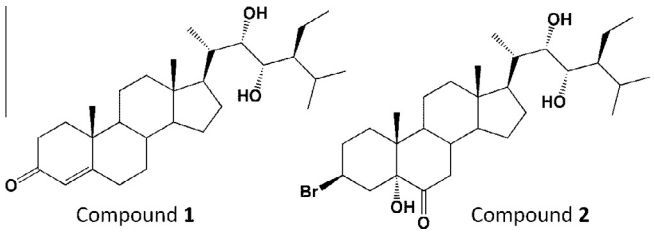

Fig. 1. Structures of compounds **1** and **2**.

LMM3 cells were seeded at a concentration of 10^4 cells/well in 96-well plates with DMEM/F12 medium supplemented with 5% FBS and they were left to adhere for 4 h. Then, the culture medium was replaced by fresh medium without serum and the cells were treated with different concentrations of compound **1** or **2** during 1, 2 or 6 h by triplicate. Supernatants were discarded, viable cells were detected by adding 10 μl MTT (5 mg/ml in distilled water) to each well and the production of formazan was evaluated by measuring the absorbance at 540 nm with an enzyme-linked immunosorbent assay (ELISA) reader (Bio-Rad Laboratories Inc., Oakland, CA) after 4 h at 37 °C. Values are mean ± S.E. and results were expressed as percentage of cell viability relative to control untreated cells.

2.3. Capillary tube formation

The formation of capillary tube-like structures by HUVEC cells was analyzed on 24-well cell culture plates, coated with an extracellular membrane matrix (Matrigel; BD Biosciences). Matrigel was thawed at 4 °C. Precooled plates and tips were used and 100 μl/well of Matrigel was distributed and allowed to jellify at 37 °C for at least 30 min. Cells were seeded on the polymerized Matrigel ($5–8 \times 10^4$ cells/well). The plate was incubated at 37 °C and tube formation was observed under an optic inverted microscope. Digital pictures were taken at different times with a camera. Tubular structures were quantified by manual counting of low power fields (25×), in at least three fields, and the percentage of inhibition was calculated with respect to untreated cells.

2.4. Cell invasion assay

HUVECs' invasion was evaluated using 24-well transwell cell culture chambers with 8 μm pore polycarbonate filter inserts. Cultured HUVECs were trypsinized and they were suspended in Medium 200, supplemented with LSGS at a concentration of 8×10^5 cells/ml. A total of 4×10^4 cell suspension was applied to insert filters. 100 ng/ml of IL-6 was used to stimulate cell migration through the inserts. For that, 600 μl of medium alone or with the stimulus in the lower chamber were added and was then incubated for 24 h at 37 °C to allow cell migration. The inserts were removed and migrated cells on the wells were fixed and stained with crystal violet. The wells were examined under a microscope. Migration was quantified by measuring the total stained cells in every well. Percent inhibition of migrating cells was calculated with respect to untreated cells.

2.5. Breast tumor angiogenesis in vivo

2.5.1. Western blot analysis of VEGF-A production by tumor cells

LMM3 cells were seeded in 6-well plates (2×10^6/well) with 1 ml of DMEM/F12 and treated with compound **1** or **2** (25 ng/μl), during 1, 2 or 6 h. Supernatants were replaced by fresh medium

for 24 h and, then, they were collected and stored at −80 °C. Protein concentration was determined by the method of Bradford [22]. Supernatants (80 μg protein/lane) were subjected to 12% SDS-PAGE minigel electrophoresis. Then, proteins were transferred to nitrocellulose membranes (BioRad) and blocked with 5% skimmed milk in 20 mM Tris–HCl buffer, 500 mM NaCl, and 0.05% Tween 20 (TBS-T), for 1 h at 20–25 °C. The nitrocellulose strips were incubated overnight with an anti-VEGF-A antibody made in rabbit (sc-1836, Santa Cruz Biotechnology Inc.), diluted 1:100 in TBS-T. After several rinses with TBS-T, strips were incubated at 37 °C for 1 h with a goat polyclonal anti-rabbit IgG conjugated with peroxidase, diluted 1:20,000 in TBS-T with 3% skimmed milk. Bands were detected by enhanced chemiluminescence. Quantification of the bands was performed by densitometric analysis using Image J program (NIH), and expressed in optical density (O.D.) units relative to original cell number.

2.5.2. Tumor induced angiogenesis assay

Tumor induced angiogenesis was quantified with an *in vivo* bioassay previously described [23]. Briefly, LMM3 tumor cells were detached and washed twice with culture medium. Cell concentration was adjusted to 2×10^6 cells/ml in DMEM/F12 medium. Cells (2×10^5/0.1 ml) were inoculated intradermically (i.d.) in each flank of BALB/c mice. On day five, animals were sacrificed and the inoculated sites were photographed under a dissecting microscope (Konus) (6.4× magnification). Images were projected on a reticular screen to count the number of vessels per mm^2 of skin (N° vessels/mm^2).

2.6. VEGF expression in J774A.1 cells

The expression vectors pVEGF-LUC (encoding firefly luciferase) and pβ-gal were kindly donated by Dr. Arzt research group (FCEyN, UBA, Argentina).

J774A.1 cells were grown to confluence in 6-well microplates and transfected with 0.5 g of pVEGF-LUC and pβ-gal plasmids, in the presence of lipofectamine (DNA lipofectamineTM 2000, InVitrogen, California, USA), diluted in the Opti-MEM medium without serum and antibiotics, according to the manufacturer's instructions. After 4–6 h of incubation at 37 °C in 5% CO_2 atmosphere, the medium was discarded and replaced by fresh Opti-MEM with 10% FBS, without antibiotics, and incubated at 37 °C in 5% CO_2 atmosphere for 24 h.

The medium was discarded and cells were stimulated with 100 ng/ml LPS and 1 ng/ml of IL-6 in Opti-MEM medium with 10% FBS. After 8 h and 16 h stimulation, the medium was discarded and the cells were lifted by scrapping in 0.1 ml per well of 1× lysis buffer. The samples were stored at −70 °C until processing.

In order to measure luciferase activity, 20 μl of each sample were mixed with 80 μl of substrate for firefly luciferase and measured in a luminometer. In the same samples, β-gal activity was measured in 96-well microplates. To do this, 20 μl of each sample were mixed with 80 μl of substrate for β-galactosidase and incubated at 37 °C until colour developed. The absorbance of these mixtures was measured at 450 nm in an ELISA reader.

We determined the expression of luciferase as a reporter of VEGF promoter activity values obtained by normalizing them against β-gal activity in relative luciferase units (RLU) for each sample.

2.7. Corneal inoculation of HSV-1

Mice were anaesthetized with ketamine (Ketalar, Parke-Davis, Morris Plains, NJ) (2 mg/mouse i.p.) and xylazine (Rompun, Mobay, Shanee, KA). The right cornea of each mouse was scratched eight times in a criss-cross pattern with a 27-gauge needle, and 5 μl of an Herpes simplex virus type 1 (HSV-1) suspension containing 2.5×10^4 PFU of virus were instilled in the cul-de-sac.

2.8. Neovascularization clinical scoring

HSV-1 infected mice exhibiting vessel enlargement with corneal invasion (10% or more) were considered positive for neovascularization. The percentage of positive animals was calculated with respect to the PBS-treated infected control.

In order to study the severity of neovascularization, a score system was established based on the percentage of neovessel invasion of the cornea, in a range of 0–4: 0, absence of neovascularization; 1, enlargement of the vessels with corneal invasion; 2, 10–30% of the cornea invaded by neovessels; 3, 30–60% of corneal invasion; 4, 60–100% of the cornea invaded by a high number of neovessels.

2.9. Statistical analysis

Statistical analysis of *in vitro* experiments was done by a Student's *t*-test.

Fisher test was used to analyze the percentage of positive animals for corneal neovascularization, with 95% confidence intervals. The severity of corneal neovascularization was analyzed by two-way ANOVA.

For the tumor induced angiogenesis assay, one-way ANOVA analysis for paired samples was used to determine the significance of differences between mean values in all control and tested samples. The analysis was complemented by using a Tukey test to compare among mean values. Differences between means were considered significant if $p < 0.05$.

3. Results

3.1. Effect of compounds **1** and **2** on capillary tube formation and cell invasion in vitro

The antiangiogenic effect of both compounds was analyzed by measuring the ability of HUVEC cells to form capillary tubes [24]. Cells were seeded on polymerized Matrigel together with different concentrations of compounds **1** and **2**. The Matrigel assay condition supported differentiation of untreated HUVECs into an extensive and complete network of capillary-like structures (Fig. 2 A).

When compound **1** was added together with HUVECs, a concentration–response inhibition profile was observed. Indeed, compound **1** led to a 59.8 ± 1.2%, 87.9 ± 6.4% and 94.4 ± 4.6% reduction of the tube-like network at 10 μM, 20 μM and 50 μM, respectively ($p < 0.01$ vs. untreated cells). The reduction was evidenced by fragments of unconnected tubes (Fig. 2D, E and F, upper photos), whereas 100 and 200 μM of compound **1** produced a complete inhibition of tube formation (Fig. 2G and H, upper photos). Similar results were obtained with compound **2**, since concentrations of 100 and 200 μM of this compound inhibited tube formation completely (Fig. 2G and H, lower photos), while 10 μM, 20 μM and 50 μM caused a reduction of 14.9 ± 6.3%, 82 ± 3% and 92.5 ± 10.6% ($p < 0.01$), respectively (Fig. 2D, E and F, lower photos).

We also investigated whether both compounds were able to disrupt capillary tubes already established on a polymerized Matrigel. Thus, HUVECs were seeded on Matrigel-coated wells and incubated for 24 h at 37 °C or until a tube-like network was developed. Afterwards, different concentrations of compounds **1** and **2** (10, 50, and 100 μM) were added and cultures were further incubated for

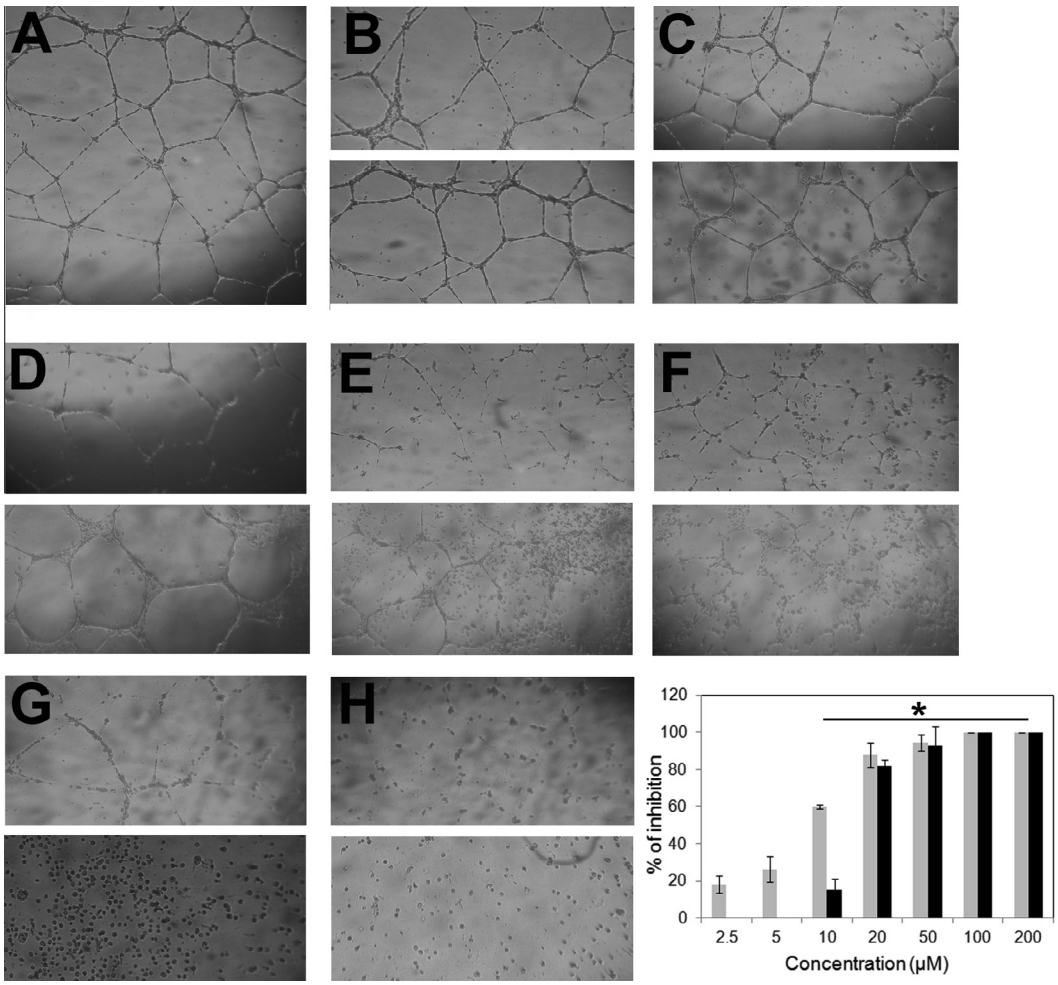

Fig. 2. Effect of compounds **1** and **2** on capillary tube formation on Matrigel. HUVEC cells were seeded on polymerized Matrigel (5–8 × 10^4 cells/well) in the presence or absence of different concentrations of compounds **1** and **2**. The plates were incubated at 37 °C, and tube formation was observed under an optic inverted microscope. Digital pictures were taken at 24 h of incubation. A: control, B–H: treatment with 2.5, 5, 10, 20, 50, 100 and 200 μM of compound **1** (upper photo) and compound **2** (lower photo), respectively. Magnification: 25×. Graph: Quantification of the inhibition of capillary tube formation (grey bars: compound **1**, black bars: compound **2**). Values are means ± SD of two experiments performed in triplicate, $^{*}p < 0.01$ vs. untreated cells.

24 h. Compound **1** did not affect the tubes already established, because no cytotoxic effect on differentiated HUVECs was observed, at any of the concentrations assayed (Fig. 3). On the contrary, compound **2** showed to be toxic at all the concentrations tested (data not shown).

As endothelial cell invasion is an initiating event critical in angiogenesis, the ability of HUVECs to migrate through a porous membrane in the presence of IL-6 was studied (100 ng/ml).

We found that IL-6 significantly enhanced cell invasion respect to non-stimulated cells (155%; $p < 0.001$) one day after cell seeding. Compound **1** efficiently suppressed HUVECs invasion when added with IL-6 in a concentration-dependent manner, given that cell migration was inhibited 18.4%, 26.1% and 67.5% at 10 μM, 20 μM and 40 μM, respectively ($p < 0.001$ vs. stimulated untreated cells). However, cell migration induced by IL-6 was not affected by compound **2** at any concentration assayed.

3.2. Effect of compounds *1* and *2* on VEGF

Given that VEGF is a primary angiogenic factor operating in the HSV-infected cornea and it is considered a target to treat corneal neovascularization, we investigated whether the compounds might exert an anti-VEGF effect *in vitro* [8,25]. Since IL-6 is involved in triggering angiogenesis through the induction of VEGF, the expression of a VEGF reporter plasmid (VEGF-LUC) was analyzed by IL-6 induction in J774A.1 cells. A β-galactosidase plasmid (β-gal) was used as a control of transfection. J774A.1 cells grown in 6-well microplates were transfected with pVEGF-LUC and pβ-gal and 24 h post-transfection, cells were stimulated with 1 ng/ml of IL-6, in the absence or presence of compounds **1** and **2** at 40 μM, concentration at which both compounds show antiviral and immunomodulatory activities *in vitro* [16–18].

In the absence of stimuli, J774A.1 cells exhibited a baseline expression of VEGF/β-gal of 13307.5 ± 3372.3 RLU. Alone, neither compound **1** nor compound **2** induced the expression of VEGF, since no significant differences were observed between its baseline expression and that obtained in the presence of the compounds (Fig. 4).

When cells were stimulated with IL-6, a significant increase in VEGF expression was observed, compared to non-stimulated control cells (30929.5 ± 5464 RLU, $p < 0.05$). Compound **1** reduced IL-6-induced VEGF expression, since it dropped to 17900 ± 2689.7 RLU ($p < 0.05$ vs. stimulated untreated cells), whereas compound **2** did not produce any significant change in VEGF expression in IL-6-stimulated cells (Fig. 4).

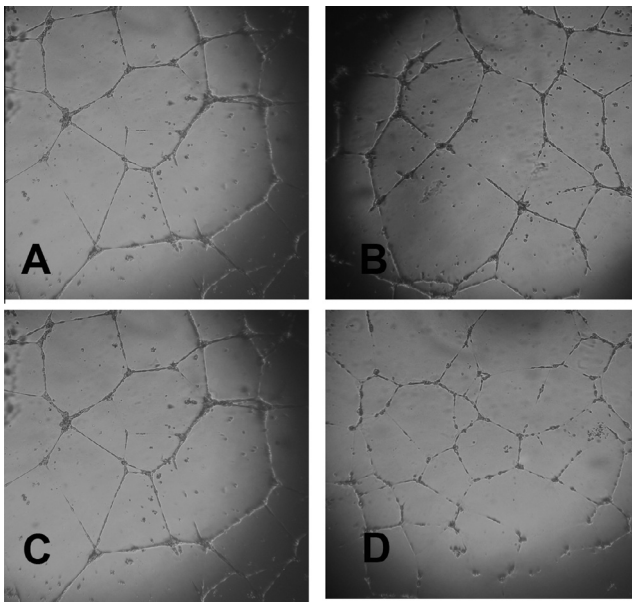

Fig. 3. Cytotoxic effect of compound **1** on already established capillary tubes on Matrigel. HUVEC cells were seeded on polymerized Matrigel ($5–8 \times 10^4$ cells/well) and the plates were incubated at 37 °C for 24 h, to allow capillary tube-like formation. The tube-like structures were incubated for further 24 h in the presence or absence of different concentrations of compound **1**. Tube-like structures were observed under an optic inverted microscope. Digital pictures were taken at 24 h of incubation. A: control, B–D: treatment with 10, 50 and 100 μM of compound **1**, respectively. Magnification: 25×.

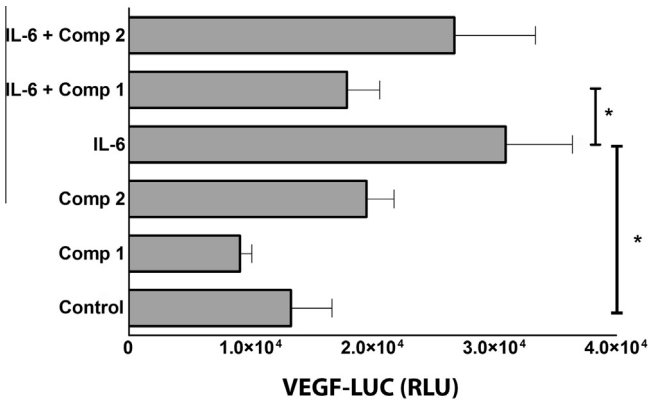

Fig. 4. Effect of compounds **1** and **2** on VEGF expression in J774A.1 cells stimulated with IL-6. Cells grown in 6-well microplates were transfected with pVEGF-LUC and pβ-gal as a control and, 24 h post-transfection, they were stimulated with 1 ng/ml IL-6 and treated or not with 40 μM of compounds **1** and **2**. After 16 h of induction, cells were harvested and luciferase expression was measured as a reporter of VEGF promoter activity. Luciferase values were normalized to β-gal activity. Control: non-stimulated transfected cells, Comp **1** and Comp **2**: non-stimulated transfected cells treated with the compounds, IL-6: IL-6-stimulated transfected cells, IL-6 + Comp: IL-6-stimulated transfected cells treated with the compounds. Values are means ± SD of two experiments performed in triplicate. $^*p < 0.05$, vs. control and vs. IL-6-stimulated cells.

3.3. Effect of compounds *1* and *2* on breast tumor cells viability

The cytotoxic effect of both compounds on LMM3 cells was investigated using MTT assay. Cells were treated with compound **1** or **2** at concentrations ranging from 12.5 to 400 μM during 1, 2 or 6 h. Cellular cytotoxicity was analyzed and expressed as a percentage of LMM3 cells without treatment. Both compounds showed a concentration-dependent effect on LMM3 cells viability (Fig. 5). The concentration 50 μM was chosen to perform the following experiments.

3.4. Effect of compounds *1* and *2* on tumor induced angiogenesis in vivo

We have previously shown that LMM3 breast tumor cells trigger a strong angiogenic response in a syngeneic model generated in BALB/c mice [23].

To study the effect of compounds **1** and **2** on the neovascular response induced by LMM3 cells in BALB/c mice, cells were treated with 50 μM of each compound, 1, 2 and 6 h prior to inoculation and, then, treated and non-treated LMM3 cells were inoculated into syngeneic mice. The anti-VEGF-A antibody Avastin was used as a control to prevent the neovascular response induced by LMM3 cells and added 2 h prior to mice inoculation.

Five days after injection, compound **1** was effective to prevent angiogenesis when added to LMM3 cells at 1, 2 and 6 h ($p < 0.01$; $p < 0.001$ vs. LMM3 cells), whereas compound **2** did not inhibit tumor induced angiogenesis at any time tested (Fig. 6A and B). As expected, Avastin exerted an inhibition of tumor induced angiogenesis in an equivalent concentration (Fig. 6A).

It is well known that LMM3 cells release high amounts of VEGF-A and express this factor in the cell membrane [23]. Thus, we studied the effect of compounds **1** and **2** on VEGF-A expression in LMM3 cells. Cells were treated with each compound (50 μM for 1, 2 and 6 h) and after incubation (24 h), supernatants were harvested and analyzed by Western blot. As shown in Fig. 6C, compound **1** inhibited the release of VEGF-A_{165} to the supernatants at all times tested. The maximal inhibitory effect of compound **1** was observed after 2 h of treatment ($p < 0.001$ vs. basal), while compound **2** showed no effect on VEGF-A_{165} secretion (data not shown).

3.5. Corneal neovascularization in HSV-1 infected mice after treatment with compounds *1* and *2*

After HSV-1 infection, corneas are invaded by neovessels, which favor the subsequent immunopathology in HSK. Hence, we evaluated if the compounds exerted an antiangiogenic effect on the HSK experimental model in mice.

At 6, 7 and 8 days after HSV-1 corneal infection, mice were treated topically three times a day with each compound, **1** and **2** (40 μM). Infected control mice received PBS. Seventy percent of the infected animals exhibited neovascularization between days 8 and 10 post-infection (p.i.) and 50% at day 14 p.i. Compound **1** reduced neovessels formation to 20% in the cornea of treated animals from day 8 to 10 ($p < 0.05$) (Fig. 7A).

A severity index of 2 was registered in infected control animals at days 8 and 10, whereas it decreased to 0.6 ($p < 0.05$) after treatment with compound **1** (Fig. 7B). Compound **2** showed no antiangiogenic effect. Therefore, we conclude that only compound **1** exerts an inhibition of corneal neovascularization when administered at the onset of HSK.

4. Discussion

Since proliferation and motility of endothelial cells are key steps of angiogenesis, these cells are attractive as a target of antiangiogenic drugs.

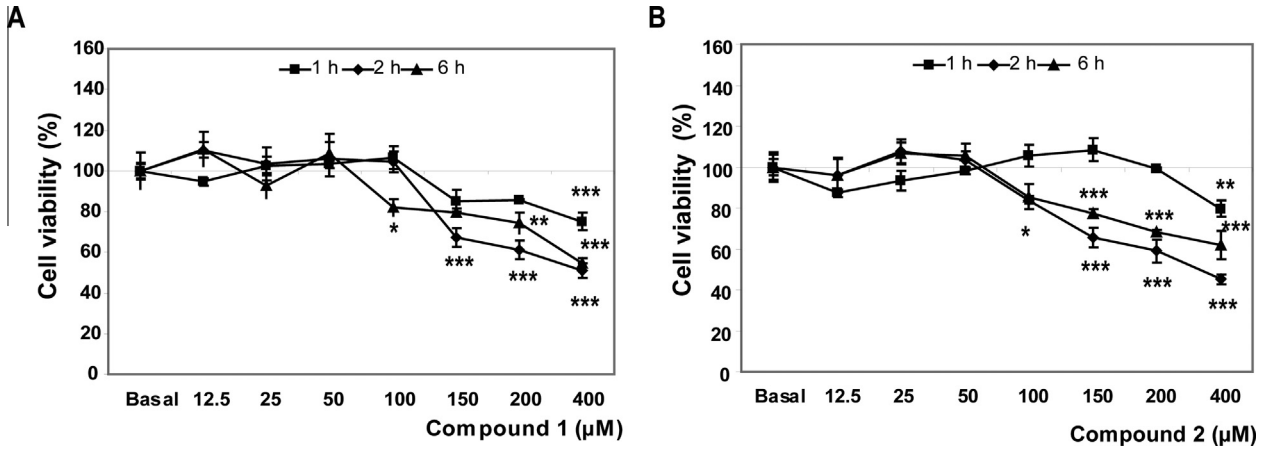

Fig. 5. Quantification of cytotoxic action of compounds **1** and **2** on LMM3 tumor. Cells (10^4 cells/well) were treated with different concentrations of compound **1** (A) or compound **2** (B) during 1, 2 or 6 h. The cytotoxic effect was analyzed after 24 h by MTT assay. Results were expressed as the percentage of cell viability respect to control (LMM3 cells without treatment considered as 100%). Values are mean ± SD of two experiments performed in triplicate. $^{*}p < 0.01$; $^{**}p < 0.001$; $^{***}p < 0.0001$ vs. basal.

In pathological situations, the angiogenic response includes VEGF as a key growth factor responsible for promoting the formation of aberrant blood vessels [26]. In the case of neovascular ocular pathologies, anti-VEGF therapies can provide substantial benefit. However, VEGF inhibition in the cancer setting is less efficient, probably due to the complexity of tumor microenvironment [26].

Although no BR with anti-VEGF bioactivity was reported, Rárová *et al.* have shown that a group of BRs can inhibit *in vitro* angiogenesis of primary endothelial cells [21].

Our previous studies described a family of 28-homobrassinosteroid analogues that share not only a wide spectrum of antiviral activity [13,15,27], but also antiinflammatory properties [17,28]. The fact that the immunomodulation exerted by these compounds resembled in part the immunomodulation provoked by glucocorticoids, led us to hypothesize that these two families of steroids might share a common mechanism of action. Nevertheless, compounds **1** and **2** are not agonists of the glucocorticoid receptor; furthermore, they are not able to inhibit the NF-κB pathway when macrophages are stimulated with several TLRs ligands, as glucocorticoids do [29]. Thus, both compounds may have a different mechanism of action from that of dexamethasone, and, eventually, would not display its undesired side effects.

The angiogenic response in ocular disease is comparable to that in cancer: VEGF regulates ocular angiogenesis through the activation and signaling of endothelial and other cell types, as it occurs in tumor angiogenesis [26]. Compound **1** proved to diminish VEGF expression when induced by IL-6, which led to inhibition of tube-like formation in endothelial cells and also of migration of these cells, two major events during angiogenesis, whereas compound **2** did not inhibit VEGF expression induced by IL-6 in macrophages (Fig. 4).

We have previously reported that compound **1** exerted an inhibitory effect on the release of IL-6 from macrophages stimulated either with LPS or TLR2 and 9 agonists [17,18,29]. Therefore, the inhibition of VEGF exerted by compound **1** could be ascribed not only to an antiinflammatory effect but also to a reduction of VEGF expression (Fig. 4) [18,29]. This property gives compound **1** an advantage over other compounds of the kind, given that some other synthetic molecules that belong to the compound **1** family, with *in vitro* immunomodulatory activity, do not have an antiangiogenic effect on the tube-like formation assay in HUVEC cells [30].

These results led us to hypothesize that compound **1** would prevent the angiogenic process by hindering endothelial cell proliferation and migration as well as through the inhibition of VEGF, or by means of a combined mechanism, which remains to be unraveled.

Results obtained with compound **1** *in vitro* correlate with findings *in vivo*. We have previously reported that compound **1** significantly ameliorates the signs of HSK when supplied either immediately after inoculation or at the onset of the disease in mice [19]. Considering that corneal neovascularization represents a key step in the blinding inflammatory HSK lesion, which usually does not resolve spontaneously, we analyzed the effect of compound **1** on the neovascularization process during murine HSK. A significant decrease in the incidence and severity of corneal neovascularization has been achieved by compound **1**, which explains the improvement of the signs of the disease already reported (Fig. 7B) [19].

Similar effects were reported with Avastin in a rabbit corneal neovascularization model, although they were observed after subconjunctival administration, an invasive ocular treatment [31,32]. Furthermore, Avastin works weakly against mouse corneal vascularization [33].

On the other hand, intraocular anti-VEGF treatment provides effective control of the human disease, although long-term intraocular injections are often required, which cause complications [24].

Regarding compound **1**, it is important to remark that the significant reduction in corneal neovascularization observed in mice was accomplished by means of a topical treatment administered when the first signs of HSK appeared. Additional benefits of compound **1** have been observed, since it exerts an antiangiogenic effect by reducing the number of neovessels in a murine model of breast cancer *in vivo* (Fig. 6).

Akt participates in the regulation of tumor growth and vascularization since it is a key molecule that controls normal and pathological angiogenesis [34]. We have previously demonstrated that compound **1** completely blocked Akt phosphorylation triggered by TLR agonists in macrophages [29]. New experiments are needed to evidence the effect of compound **1** on VEGF/Akt signaling pathway *in vivo*.

The novel antiangiogenic activity of compound **1** would be a promising alternative for the treatment of diseases where angiogenesis is one of the main pathogenic factors.

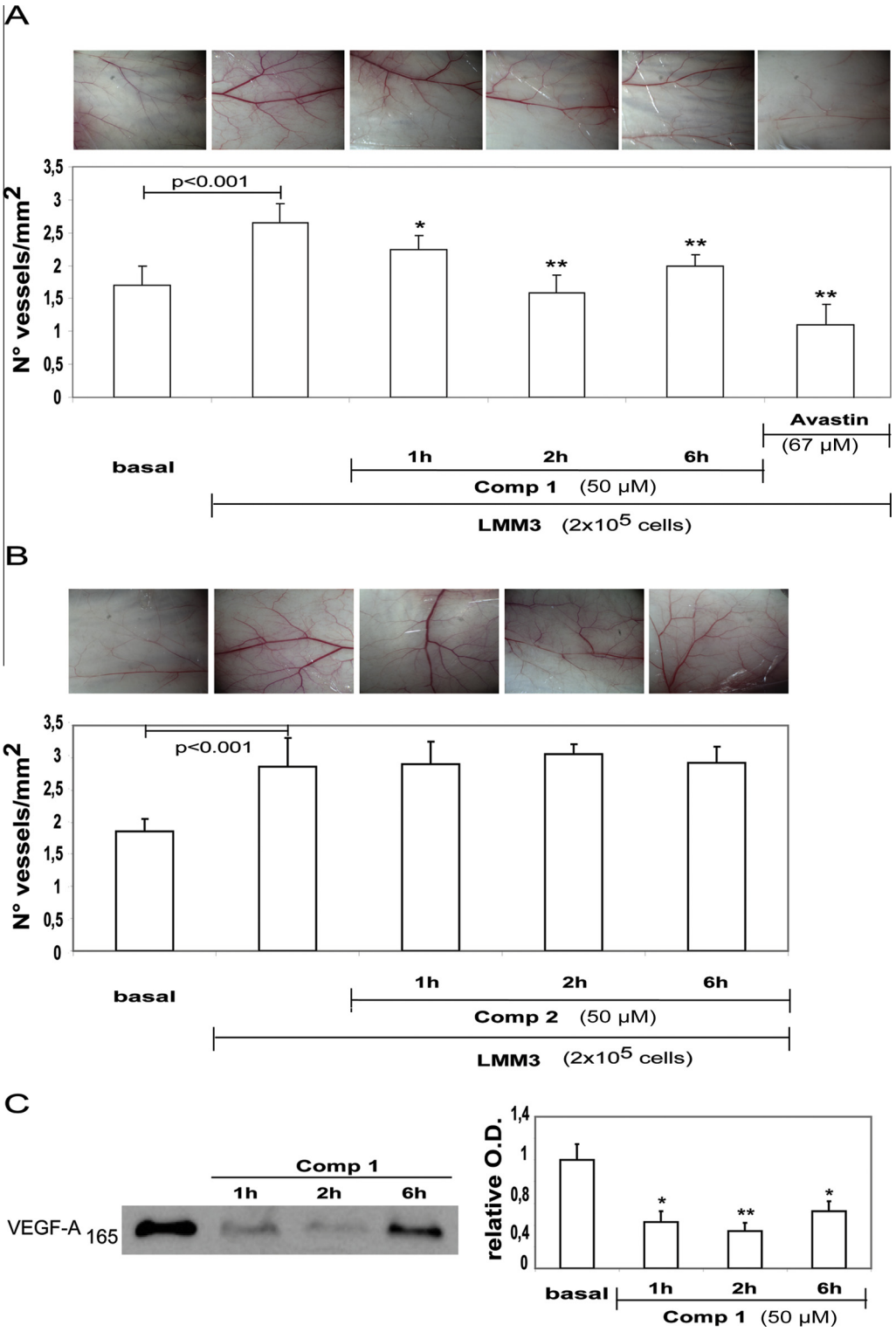

Fig. 6. (A and B) Effect of compounds **1** and **2** on tumor induced angiogenesis. Photographs of the angiogenic site for each experimental group. Magnification: 6.4× (up panels). Quantification of the neovascular response expressed as number of vessels per square millimeter of skin (N° vessels/mm^2) induced *in vivo* by 2×10^5 LMM3 cells untreated or treated with compounds **1** and **2** (50 μM) during 1, 2 or 6 h (A and B, respectively). The last bar in A is a quantification of angiogenesis of LMM3 cells treated with the anti-VEGF-A antibody Avastin during 2 h. Basal corresponds to vascular density of normal skin. Values are means ± SD of three experiments performed in triplicate. $^{*}p < 0.01$; $^{**}p < 0.001$ vs. untreated LMM3 cells (lower panel). (C) Effect of compound **1** on VEGF expression *in vivo*. Western blot assay was done to detect VEGF-A in LMM3 cell supernatants (left panel). Densitometric analysis of the bands was performed and optical density (O.D.) values were expressed with respect to basal (untreated cells considered as 1) for supernatants (right panel). Values are mean ± SD of three independent experiments. $^{*}p < 0.01$; $^{**}p < 0.001$ vs. basal.

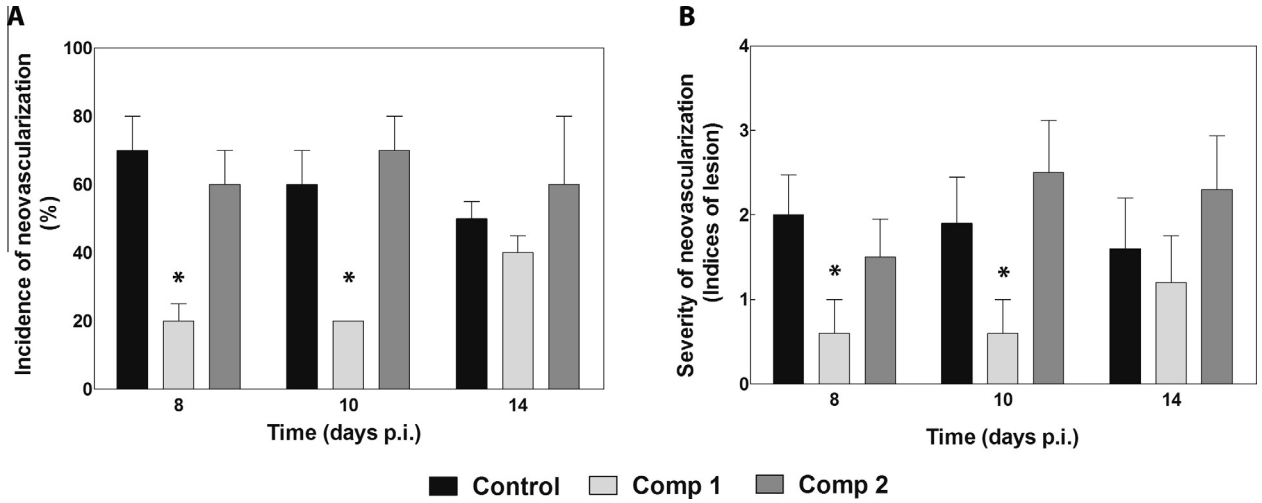

Fig. 7. Effect of compounds **1** and **2** on the evolution of corneal neovascularization. Three groups of 10 mice each were inoculated with HSV-1 KOS strain in their corneas. From day 6 p.i., each group received PBS, compound **1** (40 μM) and compound **2** (40 μM), three times a day for three consecutive days. Mice corneas were monitored for vessel enlargement and invasion until day 14 p.i. A. Incidence of neovascularization. B. Severity of neovascularization (Values are means ± SD). Data shown are representative of two experiments. $^{*}p < 0.05$ vs. infected untreated controls.

5. Conclusion

We found that compound **1**, known to display antiviral and antiinflammatory activities against HSV-1, is effective to inhibit capillary tube-like structure formation in HUVECs and the development of tumor induced angiogenesis *in vivo*. Moreover, the antiangiogenic activity of compound **1** might explain the decrease of corneal neovascularization in HSV-1-infected mice.

Here we provide direct evidence of the antiangiogenic properties of compound **1**, which widen the therapeutic potential of this compound.

6. Ethical approval

All applicable international, national, and/or institutional guidelines for the care and use of animals were followed.

Conflict of interest

The authors declare that there is no financial/commercial conflict of interest.

Acknowledgements

The authors wish to thank Dr. Javier Ramírez and Dr. Lydia Galagovsky from the Departamento de Química Orgánica de la Facultad de Ciencias Exactas y Naturales (Universidad de Buenos Aires), for kindly providing compounds **1** and **2**, and to Isabel Paz and Guillermo Assad Ferek for their technical assistance. This work was supported by grants from the Agencia Nacional de Promoción Científica y Tecnológica (ANPCyT) (PICT 0914, PICT 2010-0853), CONICET (PIP 1007), Universidad de Buenos Aires (UBACYT 20020100100522) and Instituto Massone S.A. (IMSA), Argentina.

References

[1] J.L. Owen, M. Mohamadzadeh, Macrophages and chemokines as mediators of angiogenesis, Front. Physiol. 4 (2013) 159, http://dx.doi.org/10.3389/fphys.2013.00159 (1–8).
[2] S.Y. Yoo, S.M. Kwon, Angiogenesis and its therapeutic opportunities, Mediators Inflamm. 2013 (2013) 127170, http://dx.doi.org/10.1155/2013/127170 (1–11).
[3] J. Folkman, Angiogenesis: an organizing principle for drug discovery?, Nat Rev. Drug Discov. 6 (4) (2007) 273–286, http://dx.doi.org/10.1038/nrd2115.
[4] C.T. Chen, M.C. Hung, Beyond anti-VEGF: dual-targeting antiangiogenic and antiproliferative therapy, Am. J. Transl. Res. 5 (4) (2013) 393–403.
[5] D. Ribatti, The crucial role of vascular permeability factor/vascular endothelial growth factor in angiogenesis: a historical review, Br. J. Haematol. 128 (3) (2005) 303–309.
[6] M.W. Kieran, R. Kalluri, Y.J. Cho, The VEGF pathway in cancer and disease: responses, resistance, and the path forward, Cold Spring Harb. Perspect. Med. 2 (12) (2012) 006593, http://dx.doi.org/10.1101/cshperspect.a006593 (1–17).
[7] D. Ribatti, Angiogenic activity of classical hematopoietic cytokines, Leuk. Res. 36 (5) (2012) 537–543, http://dx.doi.org/10.1016/j.leukres.2012.02.003.
[8] F. Gimenez, A. Suryawanshi, B.T. Rouse, Pathogenesis of herpes stromal keratitis–a focus on corneal neovascularization, Prog. Retin. Eye Res. 33 (1) (2013) 1–9, http://dx.doi.org/10.1016/j.preteyeres.2012.07.002.
[9] S. Kaye, A. Choudhary, Herpes simplex keratitis, Prog. Retin. Eye Res. 25 (4) (2006) 355–380, http://dx.doi.org/10.1016/j.preteyeres.2006.05.001.
[10] C. Romanutti, V. Castilla, C.E. Coto, M.B. Wachsman, Antiviral effect of a synthetic brassinosteroid on the replication of vesicular stomatitis virus in Vero cells, Int. J. Antimicrob. Agents 29 (3) (2007) 311–316. S0924-8579(06)00468-7 [pii]\r10.1016/j.ijantimicag.2006.11.005.
[11] V. Castilla, M. Larzabal, N.A. Sgalippa, M.B. Wachsman, C.E. Coto, Antiviral mode of action of a synthetic brassinosteroid against Junin virus replication, Antiviral Res. 68 (2) (2005) 88–95, http://dx.doi.org/10.1016/j.antiviral.2005.07.007.
[12] M.B. Wachsman, V. Castilla, L.B. Talarico, J.A. Ramírez, L.R. Galagovsky, C.E. Coto, Antiherpetic mode of action of (22S,23S)-3beta-bromo-5alpha,22,23-trihydroxystigmastan-6-one *in vitro*, Int. J. Antimicrob. Agents 23 (5) (2004) 524–526.
[13] M.B. Wachsman, J.A. Ramírez, L.R. Galagovsky, C.E. Coto, Antiviral activity of brassinosteroids derivatives against measles virus in cell cultures, Antivir. Chem. Chemother. 13 (1) (2002) 61–66.
[14] L.B. Talarico, J.A. Ramírez, L.R. Galagovsky, M.B. Wachsman, Structure-activity relationship studies in a set of new brassinosteroid derivatives assayed against herpes simplex virus type 1 and 2 in cell cultures, Med. Chem. Res. 11 (8) (2002) 434–444.
[15] M.B. Wachsman, E.M. López, J.A. Ramírez, L.R. Galagovsky, C.E. Coto, Antiviral effect of brassinosteroids against herpes virus and arenaviruses, Antivir. Chem. Chemother. 11 (1) (2000) 71–77.
[16] F.M. Michelini, J.A. Ramírez, A. Berra, L.R. Galagovsky, L.E. Alché, *In vitro* and *in vivo* antiherpetic activity of three new synthetic brassinosteroid analogues, Steroids 69 (11–12) (2004) 713–720, http://dx.doi.org/10.1016/j.steroids.2004.04.011.
[17] F.M. Michelini, A. Berra, L.E. Alché, The *in vitro* immunomodulatory activity of a synthetic brassinosteroid analogue would account for the improvement of herpetic stromal keratitis in mice, J. Steroid Biochem. Mol. Biol. 108 (1–2) (2008) 164–170, http://dx.doi.org/10.1016/j.jsbmb.2007.10.002.
[18] F.M. Michelini, P. Zorrilla, C. Robello, L.E. Alché, Immunomodulatory activity of an anti-HSV-1 synthetic stigmastane analog, Bioorg. Med. Chem. 21 (2) (2013) 560–568, http://dx.doi.org/10.1016/j.bmc.2012.10.054.
[19] F.M. Michelini, J.A. Ramírez, A. Berra, L.R. Galagovsky, L.E. Alché, Anti-herpetic and anti-inflammatory activities of two new synthetic 22,23-dihydroxylated stigmastane derivatives, J. Steroid Biochem. Mol. Biol. 111 (1–2) (2008) 111–116, http://dx.doi.org/10.1016/j.jsbmb.2008.05.005.
[20] J.A. Ramírez, A. Berra, F. Michelini, L. Galagovsky, L. Alché. A compound showing anti-inflammatory activity and antiviral activity, pharmaceutical compositions comprising the same, a process for obtaining the same and use of

the same in the treatment of epidemic keratoconjunctivities and herpetic stromal keratitis. US Patent N° 8431554, 2013.
[21] L. Rárová, S. Zahler, J. Liebl, V. Krystof, D. Sedlak, P. Bartůněk, et al., Brassinosteroids inhibit *in vitro* angiogenesis in human endothelial cells, Steroids 77 (13) (2012) 1502–1509, http://dx.doi.org/10.1016/j.steroids.2012.08.011.
[22] M.M. Bradford, A rapid and sensitive method for the quantitation of microgram quantities of protein utilizing the principle of protein-dye binding, Anal. Biochem. 72 (1976) 248–254, http://dx.doi.org/10.1016/0003-2697(76)90527-3.
[23] L.E. Davel, L. Rimmaudo, A. Español, E. de la Torre, M.A. Jasnis, M.L. Ribeiro, T. Gotoh, E.S. de Lustig, M.E. Sales, Different mechanisms lead to the angiogenic process induced by three adenocarcinoma cell lines, Angiogenesis 7 (1) (2004) 45–51.
[24] S. Patan, Vasculogenesis and angiogenesis, Cancer Treat. Res. 117 (2004) 3–32.
[25] P. Carmeliet, Angiogenesis in life, disease and medicine, Nature 438 (7070) (2005) 932–936, http://dx.doi.org/10.1038/nature04478.
[26] S. Moens, J. Goveia, P.C. Stapor, A.R. Cantelmo, P. Carmeliet, The multifaceted activity of VEGF in angiogenesis – implications for therapy responses, Cytokine Growth Factor Rev. 25 (4) (2014) 473–482, http://dx.doi.org/10.1016/j.cytogfr.2014.07.009.
[27] M. Wachsman, J. Ramírez, L. Talarico, L. Galagovsky, C. Coto, Antiviral activity of natural and synthetic brassinosteroids, Curr. Med. Chem.: Anti-Infect. Agents 3 (2004) 163–179.
[28] J.A. Ramírez, A.C. Bruttomesso, F.M. Michelini, S.L. Acebedo, L.E. Alché, L.R. Galagovsky, Syntheses of immunomodulating androstanes and stigmastanes: comparison of their TNF-α inhibitory activity, Bioorg. Med. Chem. 15 (2007) 7538–7544.
[29] F.M. Michelini, C.A. Bueno, A.M. Molinari, M.D. Galigniana, L.R. Galagovsky, L.E. Alché, J.A. Ramírez, Synthetic stigmastanes with dual antiherpetic and immunomodulating activities inhibit ERK and Akt signaling pathways without binding to glucocorticoid receptors, Biochim. Biophys. Acta 1860 (1 Pt A) (2016) 129–139, http://dx.doi.org/10.1016/j.bbagen.2015.10.024.
[30] J.A. Ramírez, A. Berra, F.M. Michelini, L.R. Galagovsky, L.E. Alché, Antiangiogenic brassinosteroid compounds. US Patent N° 9187518 B2, 2015.
[31] J.H. Park, C.K. Joo, S.K. Chung, Comparative study of tacrolimus and bevacizumab on corneal neovascularization in rabbits, Cornea 34 (4) (2015) 449–455, http://dx.doi.org/10.1097/ICO.0000000000000336.
[32] M. Saravia, G. Zapata, P. Ferraiolo, L. Racca, A. Berra, Anti-VEGF monoclonal antibody-induced regression of corneal neovascularization and inflammation in a rabbit model of herpetic stromal keratitis, Graefes Arch. Clin. Exp. Ophthalmol. 247 (10) (2009) 1409–1416, http://dx.doi.org/10.1007/s00417-009-1101-y.
[33] F. Giménez, A. Suryawanshi, B.T. Rouse, Pathogenesis of herpes stromal keratitis – a focus on corneal neovascularization, Prog. Retin. Eye Res. 33 (1) (2013) 1–9, http://dx.doi.org/10.1016/j.preteyeres.2012.07.002.
[34] B.H. Jiang, L.Z. Liu, AKT signaling in regulating angiogenesis, Curr. Cancer Drug Targets 8 (1) (2008) 19–26, http://dx.doi.org/10.2174/156800908783497122.